Nonlinear sublevel-coherence effects in the phase-conjugate emission of Doppler-broadened dilute media

C. Schmidt-Iglesias

Departament de Física, Universitat Autònoma de Barcelona, 08193 Bellaterra, Spain

Nonlinear effects of sublevel coherence on resonant backward-degenerate four-wave mixing are analyzed in the saturation regime of an inhomogeneously broadened and optically thin gas medium, composed of Λ-type three-level atoms. No limitations are set to the pump-field intensities, and an analytical approach is presented in the Doppler limit and efficient transverse-optical-pumping regime. It is shown that coherent population trapping due to strong pump-field coupling has a negligible incidence in phase conjugation, while interference of two imbalanced coherent-population-injection channels determines the mixing process. Level-crossing emission resonances are found to exhibit particular line-shape characteristics: (1) an insensitivity to power shifts, (2) strong power-broadening accompanied by incomplete line splitting, or (3) field-induced line-broadening inhibition. The conditions under which these effects should be observable are identified, and their dependence on pump imbalance is remarked.

I. INTRODUCTION

Resonant four-wave mixing is a subject of continued interest since the phase-conjugation experiments in vapors [1,2]. Extensive investigations have provided a lot of information on the nonlinear mixing properties of gas media and pointed out the decisive role of the atomic velocity distribution and high-order saturation effects. Particular attention is being paid to the incidence of two-photon coherence mechanisms. Phenomena arising in the saturation regime that alter the polarization properties and fidelity of vectorial phase conjugation [3], the generation efficiency, and spectral emission characteristics [4–9] allow inversionless amplification and oscillation [10,11], but also result in field-induced extra resonances [9,12] or optical bistability [13,14] have been recently reported.

Multilevel and level-degeneracy effects not only allow the possibility of both wave-front and polarization conjugation [15], but also lead to distinct nonlinear mixing mechanisms. The phase-conjugation process may often be related to the selection of a predominant optically induced population or Zeeman-coherence (ZC) grating mechanism [16] that resists the washout effects of atomic motion [17], and on which a pump beam is diffracted into the path of the signal wave. Compared to the well-studied population generation mechanism, basically analog to a saturated absorption process induced by a spatially modulated pump field [18], saturated sublevel-coherence mechanisms and their interplay with transverse optical pumping (TOP) have only begun to be explored thoroughly [4–10]. Most analyses of ZC generation mechanisms have been limited to the extent of the traditional third-order perturbation theory [16,19–22] and are often related to the study of pressure-induced extra resonances [22], where the nonresonant optical excitation does not generally induce a strong saturation or optical-pumping regime.

Reported saturation effects involving ZC mechanisms are intriguing and rather divergent. The enhanced generation of sublevel coherence through TOP is well known to originate nonabsorption resonances and dark fluorescence lines [23] or inhibition of polarization switching [13], owing to the destructive interference of two adjacent transition channels and resultant coherent population trapping [24,25]. Such nonlinear coherence effects have also been ascribed to the origin of a drastic level-crossing emission reduction [4,5], occurring already at very weak pump intensities, much lower than those required for saturation of the optical transitions. But also a complementary signal cancellation phenomenon has been recently identified, when the frequency difference of two applied fields becomes equal to the frequency splitting of the lower levels [9]. There, dipole-dipole interference does not enhance sublevel coherence, but may on the contrary annul the generation of sublevel coherence. Nevertheless, resultant line-shape splitting of level-crossing [4] or laser-frequency tuned emission resonances [9] has been predicted with simple stationary three- and four-level atom models, respectively. Such models may provide misleading conclusions in Doppler-broadened gas media as they neither account for motional washout effects nor for the directional anisotropy of saturation [26].

An unexpected sensitivity of the phase-conjugate emission (PCE) behavior to the field polarization has been lately detected, evidencing that line splitting does not always characterize the saturated response of Doppler-broadened and optically thin three-level media [7,8]. This line-shape behavior is intimately related to ZC mechanisms and has been studied in the particular case of unilateral forward [7] or backward [8] saturation, when, moreover, TOP effects are not effectively enhanced by the passive contribution of relaxation mechanisms.

In this paper, we analyze the actual incidence of nonlinear coherence and related TOP effects in the mixing process of inhomogeneously broadened three-level sys-

tems. PCE characteristics are evaluated for an optically thin medium using the framework of optical Bloch equations. We show that the population trapping coherence, avoiding saturating pump-field absorption and previously attributed to PCE inhibition [4], has a negligible incidence. A simple analytical approach that allows quantitative predictions and a clearer physical understanding of the mixing process is thus introduced. The approach is based on a single effective ZC mechanism in agreement with thermal washout effects, and has optimum validity whenever TOP dominates the effective saturation of the atomic system. PCE is shown to arise from an imbalanced ZC mechanism, basically supported by the coherent coupling of copropagating strong and weak fields that preserves the characteristic insensitivity to light shifts of coherent population trapping, but is markedly influenced by counteracting coherent-population-injection mechanisms induced by the counterpropagating pump beams. Saturation anisotropy effects such as field-induced line-narrowing mechanisms are studied in detail.

The paper is divided as follows. Section II introduces the considered degenerate four-wave mixing (DFWM) scheme and the theoretical formalism is presented in Sec. III. The general expression of the phase-conjugated field intensity is determined and the distinct contributions of atomic velocity groups are pointed out. Average over the velocity distribution is discussed and an analytical approach to the macroscopic medium response is introduced in Sec. IV. Its range of validity is established by comparison with numerical results obtained in the Dopper limit. Physical interpretations are proposed along with the simple analytical formalism and main PCE features are analyzed in Sec. V. Conclusions are presented in Sec. VI.

II. DFWM INTERACTION SCHEME

We consider a backward DFWM interaction in an inhomogeneously broadened gas medium composed of Λ-type three-level absorbers, as schematically depicted in Fig. 1. The incident laser field comprises two orthogonally polarized components $\mathbf{E}_1$ and $\mathbf{E}_2$ that respectively connect by one-photon transitions the $|1\rangle$ and $|2\rangle$ degenerate ground-state sublevels to a common upper state $|0\rangle$.

Intrinsic to the two-photon coupling of these dipole-allowed transitions is the generation of sublevel coherence that plays a decisive role in the considered mixing process. In particular, and referring to the often used grating analogy of low-power DFWM [16], the phase-conjugation process results from the diffraction of backward pump (BP) wave $\mathbf{E}_1^S$ on an atomic-motion-resistant sublevel-coherence grating, induced by the interaction of the copropagating probe $\mathbf{E}_1^N$ and forward pump (FP) wave $\mathbf{E}_2^S$ in the sample.

The mixing process is controlled by means of an external perturbation that allows the removal of the ground-state degeneracy and reduces the incidence of sublevel coherence as the splitting 2δ increases. Experimentally, this situation can be realized using the $J=1$ to $J=0$ tran-
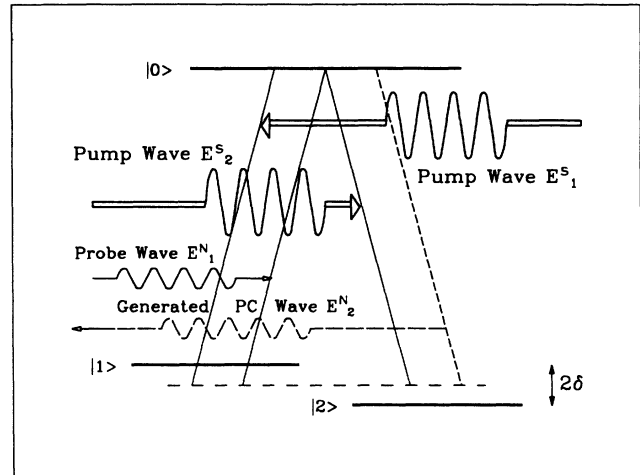
FIG. 1. Field and level configurations used in the theoretical analysis of DFWM. The forward pump interacts with the $0\rightarrow2$ transition, while the backward pump and probe waves couple only to the $0\rightarrow1$ transition. An external perturbation mechanism is allowed to induce a variable ground-state splitting 2δ.

sition of an atomic system and applying a static magnetic field, directed along the propagation axis of the orthogonally and circularly polarized fields.

The DFWM response is analyzed in a collinear laser-beam configuration in order to avoid results dominated by residual Doppler broadening. The three incident field components are thus given by

$$\mathbf{E}_1(z,t) = \sum_{T=S,N} \{ A_1^T \mathbf{e}_1 \exp[-i(Wt - \mu_1^T Kz)] + \text{c.c.} \}/2$$

(1)

and

$$\mathbf{E}_2(z,t) = \{ A_2^S \mathbf{e}_2 \exp[-i(Wt - \mu_2^S Kz)] + \text{c.c.} \}/2 ,$$

(2)

with $\mu_1^S = -1$ and $\mu_1^N = \mu_2^S = +1$, and where the superscripts S and N denote the saturating and nonsaturating waves, respectively. The detuning of the crosspolarized field components $\mathbf{E}_1$ and $\mathbf{E}_2$ is respectively defined by

$$\Delta_1 = -\delta, \quad \Delta_2 = +\delta .$$

(3)

The considered field configuration fulfills the basic requirements for vectorial phase conjugation [15] and the generated signal wave

$$\mathbf{E}_2^N = \{ A_2^N \mathbf{e}_2 \exp[-i(Wt + Kz)] + \text{c.c.} \}/2 ,$$

(4)

counterpropagating with respect to the probe beam, has the adequated polarization state $\mathbf{e}_2$ to interact only with the $0\rightarrow2$ transition.

For an optically thin sample of length L and invoking the slowly varying envelope approximation, the incident field amplitudes are almost constant along the whole sample and the weak radiated field amplitude is simply related to the induced polarization by

$$A_2^N = \frac{-iKL}{\epsilon_0} \mathcal{P}^{\text{PC}} ,$$

(5)

where $K = W/c$ is the free-space wave number and $\mathcal{P}^{PC}$ the amplitude of the phase-matched polarization component,

$$\mathbf{P}^{PC} = \mathcal{P}^{PC}\mathbf{e}_2\exp[-i(Wt + Kz)] + \text{c.c.} \tag{6}$$

III. THEORY

The considered DFWM interaction is readily treated in the semiclassical formalism of the density matrix $\rho(v,z,t)$. The evolution of an ensemble of three-level atoms with velocity v along the laser propagation axis z is described according to the master equation [27]

$$\left[\frac{\partial}{\partial t} + v\frac{\partial}{\partial z}\right]\rho_{ij} = -\frac{i}{\hbar}[H,\rho]_{ij} + \frac{d\rho}{dt}\bigg|_{\text{relax}}$$

$$(i,j = 0,1,2) , \tag{7}$$

where

$$H = \sum_{j=0,1,2} \hbar W_j |j\rangle\langle j| - \boldsymbol{\mu}\mathbf{E}(z,t) \tag{8}$$

is composed of the unperturbed atom and interaction Hamiltonian, $\boldsymbol{\mu}$ being the electric dipole moment operator with nonzero matrix elements $\langle 1|\boldsymbol{\mu}|0\rangle = \mu\mathbf{e}_1$ and $\langle 2|\boldsymbol{\mu}|0\rangle = \mu\mathbf{e}_2$. Relaxation mechanisms are accounted for in

$$\frac{d\rho}{dt}\bigg|_{\text{relax}} = \delta_{ij}(\Lambda_i - \gamma_i\rho_{ij}) - (1 - \delta_{ij})\Gamma_{ij}\rho_{ij} , \tag{9}$$

through the phenomenological population decay rates γ_j and coherence decay constants $\Gamma_{ij} = (\gamma_i + \gamma_j)/2 + \Gamma_{ij}^c$, where Γ_{ij}^c is a possible nonzero contribution due to phase-interrupting collisions. Because of lower-state sublevel degeneracy, we assume $\gamma_1 = \gamma_2 = \gamma$ and $\Gamma_{01} = \Gamma_{02} = \Gamma$. The velocity distribution of population at thermal equilibrium is established along with the incoherent pumping mechanisms described by the rates $\Lambda_j = \gamma_j N_j^e(v)$. Only the ground-state sublevels are equally population filled in the absence of optical excitation, and corresponding population differences between upper and lower levels are defined by

$$N_{0j}^e(v) = N_0^e(v) - N_j^e(v) = -P_j M(v), \quad P_1 = P_2 = P , \tag{10}$$

where $2P$ is the total density of absorbers per unit cell length and $M(v) = (\pi^{1/2}u)^{-1}\exp(-v^2/u^2)$ is the normalized velocity distribution with most probable velocity u.

The net induced polarization $\mathbf{P}(z,t)$, is given in terms of the density matrix by $\mathbf{P}(z,t) = \int_{-\infty}^{+\infty}\text{Tr}[\boldsymbol{\mu},\rho(v,z,t)]dv$, is evaluated within the standard rotating-wave approximation. The Hermitian interaction energy matrix is thus given by

$$(\boldsymbol{\mu}\mathbf{E})_{0j} = \hbar \sum_{T=S,N} \Omega_j^T\exp[i(Wt - \mu_j^T Kz)] \quad (j = 1,2) , \tag{11}$$

where, assuming an optically dilute medium that provides phase-conjugate reflectivities far less than unity, we are enabled to ignore the interaction effects induced by the generated signal wave $\mathbf{E}_2^N$. Furthermore, the penetration-depth-independent half-Rabi frequencies Ω_1^S

and Ω_2^S of the pump fields are supposed real without loss of generality. For a weak probe beam $(\Omega^N < \Omega^S)$, the equation of motion for the density matrix can be solved using the well-known semiperturbative approach of saturated-absorption spectroscopy [28]. The effect of the strong pump fields on the medium is dealt with exactly, whatever their intensity, while the interaction with the probe is described perturbatively by expanding the solution in powers of the weak-field half-Rabi frequency

$$\rho_{ij} = \rho_{ij}^{(0)} + \rho_{ij}^{(1)} + \rho_{ij}^{(2)} + \cdots \quad \text{with } \rho_{ij}^{(n)} \propto \left[\frac{\Omega^N}{\Gamma}\right]^n . \tag{12}$$

Laser interaction induces spatial modulation of populations and coherences, described through the Fourier components

$$\rho_{ij}^{(p)}(v,z,t) = \exp[-iWt(\delta_{0,i} - \delta_{0,j}) + i(\mu_i^S - \mu_j^S)Kz]$$

$$\times \sum_{m \leq 2p} \rho_{ij(m)}^{(p)}(v)\exp(imKz) , \tag{13}$$

$$\rho_{ij(m)}^{(p)} = (\rho_{ij(-m)}^{(p)})^*, \quad i,j = 0,1,2 , \tag{14}$$

where $\mu_0^S = 0, \delta_{0,j}$ are Dirac functions, and $\rho_{ij(m)}^{(p)}$ are nonvanishing coefficients as long as the integers m are even.

The present formalism allows an iterative determination of the atomic response to any desired order in the probe strength (see Appendix). But for a nonsaturating probe beam, calculations up to first order yield already the steady-state polarization term P^{PC} of Eq. (6), and the emitted field intensity acquires the expression

$$I^{PC} = |\mathbf{A}_2^N|^2 = \left|\frac{-iKL}{\epsilon_0}\mu\mathbf{e}_2\langle\rho_{02(-2)}^{(1)}\rangle\right|^2 , \tag{15}$$

where the $\langle\ \rangle$ symbol denotes the velocity average.

The mixing response due to the distinct atomic velocity groups may be decomposed into three physically distinguishable contributions

$$\rho_{02(-2)}^{(1)} = \rho_Z + \rho_C + \rho_H , \tag{16}$$

defined by

$$\rho_Z = \frac{i\sqrt{I_1 I_2}\,\Omega_1^{N*}}{(1 - i\delta_2^-)\Gamma}\frac{D_1^{+*}N_{01(0)}^{(0)} + D_2^+ N_{02(0)}^{(0)}}{Z^{++}} , \tag{17}$$

$$\rho_C = \frac{-i\Omega_1^{N*}}{(1 - i\delta_2^-)\Gamma}N_{02(-2)}^{(1)} \tag{18}$$

$$\rho_H = \frac{iI_1\Omega_1^{N*}}{(1 - i\delta_2^-)\Gamma}\left[\frac{D_1^{+*}N_{01(-2)}^{(1)} + D_2^- N_{02(-2)}^{(1)}}{Z^{++}}\right.$$

$$\left. - \frac{\sqrt{I_1 I_2}}{(1 - i\delta_2^+)}\frac{D_1^{-*}N_{01(0)}^{(0)} + D_2^+ N_{02(0)}^{(0)}}{Z^{-+}Z^{++}}\right] , \tag{19}$$

where the Fourier components of the population differences

$$N_{0j}^{(p)}(v,z,t) = \rho_{00}^{(p)} - \rho_{jj}^{(p)} = N_{0j(m)}^{(p)}(v)\exp(imKz) \tag{20}$$

indicate with $m = (\mu_1^S - \mu_1^N) = -2$ the influence of the spatial inhomogeneity induced by the quasistanding wave $\mathbf{E}_1$. The dimensionless detuning parameters are defined by

$$\delta_j^\mu = (\Delta_j - \mu K v)/\Gamma , \tag{21}$$

$$D_j^\mu = (1 + i\delta_j^\mu)/[1 + (\delta_j^\mu)^2] , \tag{22}$$

and the saturation denominators

$$Z^{\mu\nu} = 1 + C + \frac{i(\delta_1^\mu - \delta_2^\nu)\Gamma}{\gamma} + I_1 D_2^{-\mu} + I_2 D_1^{\mu*} \tag{23}$$

with

$$C = \Gamma_{12}^C/\gamma \tag{24}$$

describe the resonance behavior of the ZC induced by the crosspolarized $\mathbf{E}_1$ and $\mathbf{E}_2$ field components, μ and ν being either positive or negative signs in correspondence with the propagation direction of the coupled field components. The normalized pump intensities

$$I_j = \frac{|A_j^S|^2}{I_S} = \frac{|\Omega_j^S|^2}{r\gamma_0\Gamma} \tag{25}$$

with

$$r = \frac{\gamma}{\gamma_0} \tag{26}$$

clearly express the influence of TOP on the effective saturation intensity I_S of the three-level system. In particular, if $r \ll 1$ is satisfied, accumulation of atoms in a coherent superposition state of the ground sublevels always dominates over the optical transition saturation, which only begins to be appreciable when $I_j^{OP} = 2rI_j = 1$ [29].

Two of the above-indicated mixing contributions can be related to the low-power grating generation mechanisms [16]. In particular, the first term ρ_Z describes for $I_1, I_2 \ll 1$ the so-called ZC grating mechanism induced by the copropagating incident waves. The second term ρ_C accounts for a saturated cross-population grating mechanism. Of course, the physical picture of isolated grating contributions with a well-defined interaction ordering (grating formation and subsequent readout of the grating) is not well adapted for strong saturating pump fields. In fact, sublevel coherence induced by the two saturating pump fields and resultant coherent population trapping may affect both ρ_Z and ρ_C contributions. Additional saturation effects, as high-order contributions owing to the interplay between Zeeman coherence and modulated population mechanisms, also intervene and are reckoned with in the third term ρ_H.

In order to assess the different incidence of the mixing contributions as well as the distinct role of sublevel coherence effects, Fig. 2 illustrates the spectral profile of the individual contributions as a function of the normalized atomic velocity Kv/Γ. Characteristic TOP effects are enhanced by subjecting a degenerate three-level system ($\delta = 0$) with small lower- to upper-level relaxation ratio ($r = 0.01$) to the resonant irradiation of two equally saturating pump waves ($I_1 = I_2 = 2$). The coherent
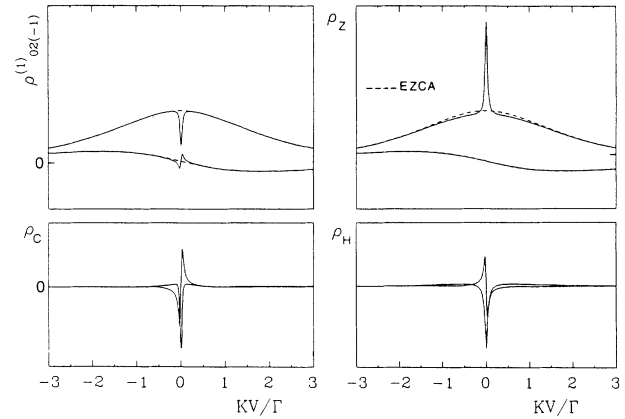
FIG. 2. The total $\rho_{02(-2)}^{(1)}$ and partial ρ_Z, ρ_C, ρ_H, mixing contributions are separately shown as a function of the normalized velocity Kv/Γ, for the case of exactly resonant fields $\Delta_1 = \Delta_2 = 0$ and equal forward and backward pump saturation parameters $I_1 = I_2 = 2$. The medium is characterized by a decay ratio $r = 0.01$ in order to enhance the efficiency of TOP and point out the influence of different nonlinear sublevel-coherence effects.

pump-field coupling clearly affects all mixing contributions, but is only effective on stationary or very slow atoms that do not detect during their field coupling time $t_c = 1/\gamma$ the difference between the Doppler-shifted frequencies of the two counterpropagating pump waves. The tuning behavior of this ZC resonance is basically characterized by the denominator Z^{-+} of Eq. (23), which exhibits the resonance condition $\delta_1^- - \delta_2^+ = 0$ and an effective half-width of $|Kv|_{eff} \leq \frac{1}{2}\gamma(1 + I_1 + I_2)$. This strong and velocity-dependent TOP resonance enhances ρ_Z, but also coincides with the opposition of phase in ρ_C. Its overall effect, including ρ_H, is to diminish the mixing contribution of slow atoms. In point of fact, during γ_0/γ successive optical interactions, the strong and balanced pump-field coupling leads to the accumulation of an increasing number of slow atoms in a pure coherent superposition state of the ground levels, in which they are no longer eligible to absorb the pump fields and thus do not contribute to PCE. This coherent population trapping effect is responsible for a drastic reduction of line-center PCE and for the predominant dispersive character of level-crossing resonances in stationary three-level systems with $r < 1$ [4].

This mixing inefficiency increases with pump intensity and is most pronounced when $I_1 = I_2$, that is, when both pump fields are subjected to an equal absorption reduction due to balanced TOP among the two ground levels. However, a striking feature at first sight is that PCE never completely annuls at line center due to a coexisting sublevel coherence induced by FP and probe beams. High atomic velocity groups also contribute to PCE via this Doppler-free coupling, accounted for in ρ_Z. This much weaker but atomic-motion-resistant ZC is thus expected to dominate the velocity-averaged mixing response. Due to the coupling of a strong and a weak field, imbalanced depopulation-pumping mechanisms are foreseen to affect PCE. It should be noted that inherent

to this imbalanced ZC is a strong decrease of the weak probe field absorption. These nonabsorption resonances affecting only the nonsaturating fields actually allow coupled-mode oscillation [30] in an absorbing optically thick medium [10].

IV. ANALYTICAL APPROACH TO THE DFWM RESPONSE

When the exact form of $\rho_{02(-2)}^{(1)}$ [Eqs. (16-19)] is used to obtain the emitted field amplitude [Eq. (15)], a numerical Doppler integration is required. But as inferred from Fig. 2, strong velocity-dependent nonlinear coherence effects may basically average to zero in an inhomogeneously broadened medium, even in the case of very high pump intensities. The behavior of PCE may be thus de-

scribed by $\langle \rho_Z \rangle$, whenever the coherent population trapping effects due to pump-field coupling are here also excluded (see dashed lines of Fig. 2). Within this "effective ZC approximation" (EZCA), zero-order population differences evolve according to the superimposed optical excitation of both dipole-allowed transitions. In particular, they are characterized by

$$N_{0j(0)}^{(0)} = \frac{N_{0j}^e[1+2(1+r)I_{3-j}^D]-N_{03-j}^e 2rI_{3-j}^D}{[1+2(1+r)I_j^D][1+2(1+r)I_{3-j}^D]-4r^2I_{3-j}^D I_j^D} ,$$

(27)

where the velocity-dependent pump-field coupling terms have been neglected (see Appendix for details). The simplified PCE contribution is thus given by

$$\langle \rho_Z \rangle_{EZCA} = \frac{1}{\sqrt{\pi}Ku} \int_{-\infty}^{+\infty} \frac{\exp[(Kv/Ku)^2]}{\Gamma(1-i\delta_2^-)} P_T \frac{i\Omega_1^{N*}\sqrt{I_1 I_2}}{\gamma[1+C+i(\Delta_1-\Delta_2)/\gamma+I_1(1-i\delta_2^-)^{-1}+I_2(1+i\delta_1^+)^{-1}]} dKv , \quad (28)$$

where

$$P_T = \frac{-P[(1+2I_2^D)(1+i\delta_1^+)^{-1}+(1+2I_1^D)(1-i\delta_2^+)^{-1}]}{1+2(1+r)(I_1^D+I_2^D)+4(1+2r)I_1^D I_2^D}$$

(29)

with $P=P_1=P_2$ acquires for $r \ll 1$ the simple form

$$P_T = \frac{-P_1}{(1+2I_1^D)(1+i\delta_1^+)} + \frac{-P_2}{(1+2I_2^D)(1-i\delta_2^+)} , \quad (30)$$

and the intensity parameters

$$I_1^D = I_1/[1+(\delta_1^-)^2], \quad I_2^D = I_2/[1+(\delta_2^+)^2] \quad (31)$$

take into account the decrease of saturation with the optical detuning δ_j^μ.

In order to illustrate the validity range of the EZCA approximation, EZCA results and the complete $\langle \rho_{02(-2)}^{(1)} \rangle$ DFWM response are plotted together in Fig. 3 as a function of the normalized pump intensity $I_P = I_1 = I_2$. A large Doppler width of $Ku = 800\gamma_0$ has been considered in order to avoid finite velocity distribution effects. Comparison directly reveals that EZCA results are markedly close to the exact solutions, to an exceptional degree when $r \ll 1$. Coherent population trapping due to balanced pump-field coupling has indeed, even at extremely high normalized pump intensities $(I_p \sim 10^3)$, a negligible incidence. Moreover, the counteracting crosspopulation grating mechanisms do not effectively contribute to DFWM whenever collisional relaxation of ZC is small and saturation of the optical transition does not participate in the nonlinear interaction. This is readily satisfied in various experimental situations, particularly when the lower levels correspond to the ground state of the system. In point of fact, phase-perturbing collisions generally have a major effect on the optical coherences, but these do not alter the validity of EZCA.

Insofar as we are interested in nonlinear coherence effects, we restrict the following analysis to the case of $r \ll 1$ and $\langle \rho_Z \rangle_{EZCA}$ acquires a simple analytically tractable expression in the Doppler limit. Velocity integration is straightforwardly performed by using the residue method [27] to give

$$\langle \rho_Z \rangle_{EZCA} = \frac{2i\sqrt{\pi}}{Ku} \sqrt{I_1 I_2} \frac{\Omega^{N*}}{\Gamma} \sum_{j=1,2} T_j , \quad (32)$$

composed of two terms:

$$T_1 = \frac{P_1 I_1}{S_1(1+S_1+2i\Delta_1/\Gamma)[1+S_1+i(\Delta_1-\Delta_2)/\Gamma]Z_1} , \quad (33)$$

$$T_2 = \frac{-P_2(1+S_2)}{2S_2(1+S_2-2i\Delta_2/\Gamma)Z_2} , \quad (34)$$

where the saturation parameters S_j are given by

$$S_j = \sqrt{2I_j+1} \quad (35)$$

and the Zeeman coherence resonance denominators Z_j by

$$Z_1 = 1 + C + i(\Delta_1-\Delta_2)/\gamma + \frac{I_1}{1+S_1+i(\Delta_1-\Delta_2)/\Gamma}$$

$$+ \frac{I_2}{1+S_1+2i\Delta_1/\Gamma} , \quad (36)$$

$$Z_2 = 1 + C + i(\Delta_1-\Delta_2)/\gamma + \frac{I_1}{1+S_2-2i\Delta_2/\Gamma}$$

$$+ \frac{I_2}{1+S_2+i(\Delta_1-\Delta_2)/\Gamma} . \quad (37)$$

Two remarkable PCE characteristics are clearly revealed. First, directional anisotropy of saturation inherent to Doppler-broadened media naturally appears through the
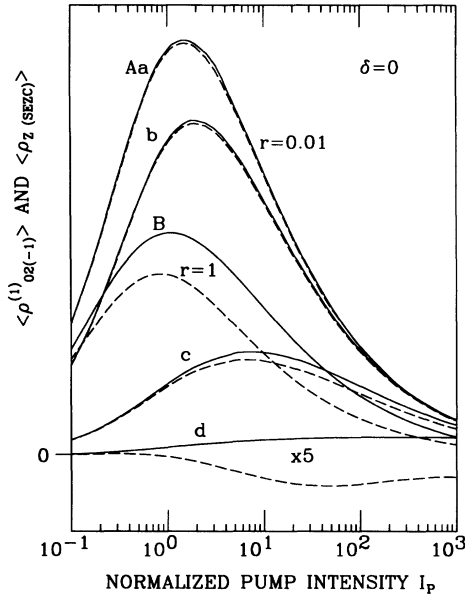
FIG. 3. Comparison between the PCE amplitudes obtained either through the analytical determination of $\langle \rho_Z \rangle_{EZCA}$ (solid curves) or the numerical evaluation of the exact $\langle \rho_{02(-2)}^{(1)} \rangle$ mixing response (dashed curves). The comparison is realized as a function of the normalized pump intensity $I_P = I_1 = I_2$ for the case of $\delta = 0$. Each pair of dashed and solid-lined curves is distinguished by (A) $r = 0.01$ and (B) $r = 1$. The effects of collisional dephasing on the Zeeman coherence is considered in case A and the a–d curves illustrate their incidence, as the dephasing rate C takes, respectively, increasing values of $C = 0$, $\gamma/2$, 8γ, and 400γ. For the high dephasing rate of $C = 400\gamma$, PCE is extremely small and mainly originates from a weak cross-population grating mechanism that counteracts the almost vanishing Zeeman-coherence contribution. The numerically evaluated $\langle \rho_{02(-2)}^{(1)} \rangle$ emission amplitude thus changes sign.

terms T_1 and T_2. In particular, T_1 only presents an appreciable contribution for an intense BP, while T_2 can be directly related to the basic generation mechanism as it always contributes to PCE, whatever the degree of pump saturation is. Moreover, since T_1 and T_2 respectively describe the different weight of P_1 and P_2 equilibrium populations participating in the ZC, they also account for counteracting FP and BP population mechanisms that, even in the absence of optical transition saturation, intervene in the mixing process. In fact, through successive optical interactions during the sublevel coherence build-up time $1/\gamma$, the E_j^S pump waves are able to deplete the j ground level and inject some P_j population in the effective sublevel coherence. The two injection mechanisms interfere destructively and may thus lead to a decrease of the generation efficiency. The described interference phenomenon is complementary to the destructive dipole-dipole interference that results in an enhancement of sublevel coherence and coherent population trapping [24,25]. It should also be distinguished from lately reported complementary dipole-dipole interferences leading to sublevel coherence cancellation [9]. Here, cancellation requires that both sublevel populations simultaneously participate in the interferencial mechanism, and

would furthermore only occur in the case of $P_1 > P_2 > 0$.

Second, the quantities Z_j manifest a characteristic tuning dependence. Specifically, Eqs. (36) and (37) exhibit the resonance conditions

$$0 = \Delta_1 - \Delta_2 + \delta_j \tag{38}$$

with power shifts δ_j given by

$$\delta_1 = \frac{2|\Omega_1^S|^2 \delta}{\Gamma^2(1+S_1)^2 + 4\delta^2} + \frac{2|\Omega_2^S|^2 \delta}{\Gamma^2(1+S_1)^2 + 4\delta^2}, \tag{39}$$

$$\delta_2 = \frac{2|\Omega_2^S|^2 \delta}{\Gamma^2(1+S_2)^2 + 4\delta^2} + \frac{2|\Omega_1^S|^2 \delta}{\Gamma^2(1+S_2)^2 + 4\delta^2}. \tag{40}$$

PCE is not sensitive to unequal light shifts of the ground sublevels induced by an imbalanced pump irradiation ($I_1 \neq I_2$), and is thus always centered at $\delta = 0$. This insensitivity to light shifts is a well-known characteristic of atoms evolving in a coherent trapping state, in which they are hindered to participate in a resonant two-photon transition. The imbalanced effective ZC retains this level-shift insensitivity, although pure coherent population trapping ($\rho_{12}\rho_{21} \sim \rho_{11}\rho_{22}$) is not involved. Nevertheless, partial trapping effects do occur, while injection-depopulation mechanisms tend to maintain a definite distribution of population between the lower levels, in accordance with the distinct ground-level depletion induced by the pump fields.
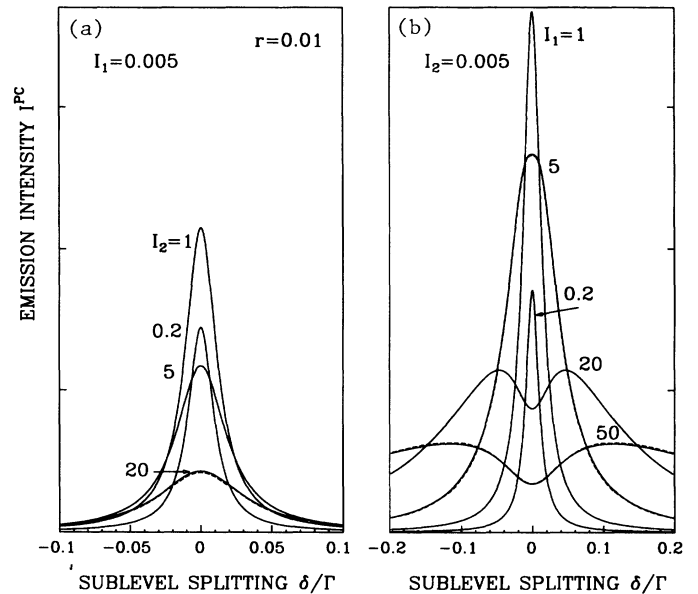
FIG. 4. Phase-conjugate intensity line shapes obtained, in the case of a single saturating pump beam, by varying the sublevel splitting δ/Γ. Unilateral saturation effects are shown in graph (a) for various normalized forward pump intensities I_2 and in (b) for distinct backward pump intensities I_1. Due to an increased scattering efficiency, higher overall PCE efficiencies are clearly obtained for the case of an intense backward pump, in spite of the central saturation dip. Dashed and solid curves correspond, respectively, to numerical and analytical solutions as in Fig. 3.
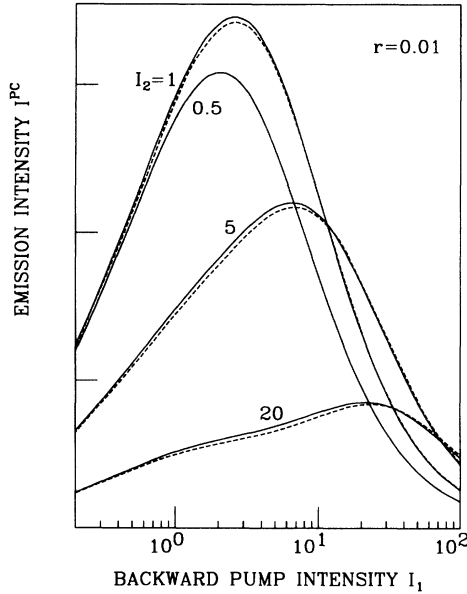
FIG. 5. Illustrating the effect of pump imbalance on TOP-affected phase conjugation. The line-center emission intensity is plotted as a function of the normalized forward pump intensity I_2 for several values of the backward pump intensity I_1. For comparison purposes with Fig. 4, a linear scale factor of $F = 50$ has to be considered, since higher generation efficiencies are obtained with bilateral saturation.

FIG. 6. Illustrating counterphase effects induced by a saturating backward pump. (a) Line shapes correspond to $I_1 \leq I_2$, and (b) curves correspond to $I_1 \geq I_2$. Note the peak enhancement and the absence of line broadening as I_1 approaches I_2. A narrow central saturation dip appears only when I_1 surpasses I_2. The comparative scale factor with respect to Fig. 4 is $F = 12.5$ in (a) and $F = 25$ in (b).

V. PCE CHARACTERISTICS

Typical counterphase injection effects on the phase-conjugate intensity line shapes are analyzed for the case of $r = 0.01$ and $Ku = 800\gamma_0$. Figures 4–6 graphically summarize the main characteristics obtained in the EZCA approximation (continuous lines), which excellently reproduces the numerically evaluated exact DFWM response (dashed lines) in the considered Doppler limit. Direct observation clearly reveals the peculiar saturation asymmetry due to competition between FP- and BP-induced counterphase mechanisms, which not only results in different PCE efficiencies but also in distinct line-shape structures.

At predominant FP saturation, the PCE line shapes remain always single peaked, while the usually expected saturation dip (always occurring in case of predominant saturated population grating mechanisms) only appears when BP is the most intense laser beam. A striking feature is moreover that line-center PCE efficiency is higher in the case of backward than in that of forward saturation, in spite of the developing saturation dip (see Fig. 4). This increased generation efficiency at predominant BP saturation prevails even at high pumping intensities, when the overall PCE strongly decreases because of important saturation effects. As a matter of fact, the saturation dip never results in a fully resolved splitting of the line. Asymmetric saturation effects are further illustrated in Fig. 5, where the line-center PCE is plotted as a function of I_1 for several values of the FP intensity I_2. As usual in phase conjugation, maximum efficiency is however reached when both pump intensities are of the

order of the normalized saturation intensity, and PCE peaks here when $I_1 > I_2 \sim 1$.

An insight into the observed saturation phenomena is gained through the T_1 and T_2 terms of $\langle \rho_Z \rangle_{EZCA}$. In the considered first-order treatment, the effective ZC mechanism is not affected by the weak probe beam population contributions. ZC buildup is thus on one side basically determined by a coherent P_2 population injection induced by FP, which may be extremely small in the case of nonsaturating FP. But since FP directly participates in the atomic-motion-resistant ZC grating, it is also able to induce strong saturation effects. With an increase of FP intensity, more P_2 atoms participate in the coherence buildup and PCE efficiency increases as I_2 tends towards 1. But for $I_2 > 1$, saturation rapidly broadens and flattens the ZC and consequently the PCE resonance. In particular, the full width at half maximum (half-width) of the T_2 contribution to the emission resonance is given through Z_2 by

$$\gamma_{(T_2)} = \gamma \left[1 + C + \frac{I_1 + I_2}{1 + \sqrt{1 + 2I_2}} \right]. \qquad (41)$$

It exactly describes the half-width of the single-peaked PCE resonance in the case of $I_1 \ll 1$. Also, if hypothetically the equilibrium population difference N_1^e of the diffracting transition (transition to which the diffracting pump beam is coupled) is zero, so that no net population changes can be induced by BP, PCE at the coupled transition remains single peaked and exhibits the half-width $\gamma_{(T_2)}$, which includes the nonlinear coherence effects of BP saturation through I_1.

But the generation mechanism is on the other side sub-

jected to important counteracting population injection effects induced by BP and described through term T_1. However, as clearly seen from Eq. (31), BP saturation effects have, in contrast to T_2, a higher atomic velocity dependence and thus a limited incidence. As easily deduced from Eqs. (33) and (34), a saturation dip reaches at the very most the half maximum of the basic T_2 contribution, i.e., $T_{1\max} \simeq -T_2/2$ at line center, particularly when only BP strongly saturates the medium and collisional dephasing of the ZC is absent ($C = 0$).

Spectral characteristics originated from the counterphase effects are fundamentally described by Z_1 of T_1 and the width of the narrow central dip approaches

$$\gamma_{(T_1)} = \gamma \left[1 + C + \frac{I_1 + I_2}{1 + \sqrt{1 + 2I_1}} \right] . \tag{42}$$

Of course, the detectability of the dip is strictly determined by the ratio of line center T_1 and T_2 amplitudes or, equivalently, by the condition $\gamma_{(T_2)} > \gamma_{(T_1)}$ fulfilled whenever $I_1 > I_2$.

A remarkable feature due to BP saturation effects is however a strong peak enhancement accompanied by line-narrowing mechanisms. This occurs when $1 < I_1 < I_2$ and $C \sim 0$ as shown in Fig. 6(a). In particular, as BP intensity is increased above saturation level towards a high FP saturation intensity, the PCE resonance is subjected to power-broadening inhibition effects and maintains the half-width

$$\gamma^{ef} \simeq \left[1 + \frac{I_2}{1 + \sqrt{1 + 2I_2}} \right] . \tag{43}$$

Important power-broadening effects described by $\gamma_{(T_2)}$ only become effective when I_1 approaches I_2 and $I_1 \geq I_2$. This particular behavior is easily understood on the basis of the following summary of BP saturation effects. On one hand, BP power enlarges the atomic velocity band that resonantly interacts with the counterpropagating diffracting and grating waves. The T_2 contribution is thus enhanced due to the increased diffraction efficiency of intense BP into the path of the signal wave. On the other hand, counterphase coherence effects supported by the diffracting ground-level population reduce through T_1 the basic ZC mechanism. At comparatively moderate BP saturation ($I_1 < I_2$), the increase of diffraction efficiency dominates over the counterphase mechanism, which primarily affects the most saturated resonant atomic groups. This naturally implies that power-broadening effects on the PCE resonance are reduced. At high BP saturation, destructive interference effects are strong enough to induce a narrow saturation dip as observed in Fig. 6(b).

VI. CONCLUSION

In this paper, we have studied the influence of nonlinear coherence effects on the PCE line shapes. Particular attention is paid to optically dilute media, where saturation of the coupled optical transitions is overwhelmed by TOP. We introduced in this situation a very simple

analytical treatment, demonstrating that nonabsorption resonances of the counterpropagating pump fields have a negligible incidence in the Doppler limit, even at very high pump intensities. The PCE process is thus not cancelled, and the absorption of two photons of the pump beams and subsequent emission of two photons in the weak phase-conjugated field modes is not hindered.

The main conclusion is that all the most interesting features pointed out here can be interpreted in terms of two counteracting coherent-population-injection mechanisms, induced by either pump field, and where the choice of pump intensity imbalance allows the degree of interference between the two mechanisms to vary. As a result, for BP < FP saturation, single-peaked and even line-narrowed resonances occur, while for BP > FP saturation a narrow central dip appears in the level-crossing PCE spectrum. An interesting point to note is that both the asymmetric and counterphase characters of the two generation contributions arise from atomic motion. Therefore total cancellation of line-center PCE does not occur in the case of stationary atoms [4].

The characteristic absence of complete line splitting due to sublevel-coherence generation mechanisms has been also confirmed in previous experimental studies of backward DFWM with weak crosspolarized grating waves and a single saturating BP [8]. However TOP was ineffective there and the distinct role of ZC and population grating mechanisms could not be distinguished. In fact, reported comparatively low PCE efficiencies may now be ascribed to saturated population grating mechanisms, which always counteract the sublevel-coherence generation process, and have an important incidence when saturation of the optical transition also participates in the mixing process. Higher PCE efficiencies with weak pump fields of several milliwatt power, can be actually obtained in the TOP regime. Moreover, the prediction of a saturation-induced line-narrowing mechanism accompanies with signal peak enhancement would be only observable under efficient TOP conditions.

Examples of atomic systems with degenerate ground states that offer the experimental opportunity to study the quantitative predictions in the TOP regime are provided by the $^7F_1 \rightarrow {}^7F_0^0$ 570.68-mn transition of Sm I vapor or by the D_1 transition in Na (though the Na level structure is not simple, it is often considered as a Λ-type three-level system [5,23]). However, our predictions cannot be directly applied to the PCE studies performed earlier in atomic sodium by Mlynek et al. [5], where due to a different adopted field polarization scheme all the fields basically interact with both coupled transitions and different nonlinear coherence effects compete.

We have focused our attention on the usual field configuration of phase conjugation using two strong counterpropagating pump waves, and a signal wave that is vectorially phase conjugated with respect to a weak probe beam is the analyzed response. Nevertheless, the present study suggests that higher mixing responses should be obtained in the complementary diffraction setup, where the grating waves have comparable saturation intensities and the diffracting beam is weak. In fact, counterphase effects would be thus eliminated and only a

C. SCHMIDT-IGLESIAS

strong balanced coherent trapping grating would come into effect. This situation requires, however, numerical evaluations and is planned to be reported in the future. An additional extension would be, of course, the case of four arbitrarily intense waves, of particular interest in intrinsic optical bistability.

APPENDIX

The iterative formalism that allows a calculation of the atomic response to any desired order in the weak-field strength is based on the following set of linear equations for $j = 1, 2$:

$$\rho_{0j(m)}^{(p)} = -iR_{0j}^{m}[\Omega_j^S N_{0j(m)}^{(p)} + \Omega_j^N N_{0j(m-n)}^{(p-1)} - \Omega_{3-j}^S \rho_{3-jj(m)}^{(p)} - \Omega_{3-j}^N \rho_{3-jj(m+n)}^{(p-1)}] , \tag{A1}$$

$$\rho_{j0(m)}^{(p)} = iR_{j0}^{m}[\Omega_j^S N_{0j(m)}^{(p)} + \Omega_j^{N*} N_{0j(m+n)}^{(p-1)} - \Omega_{3-j}^S \rho_{3-jj(m)}^{(p)} - \Omega_{3-j}^{N*} \rho_{3-jj(m-n)}^{(p-1)}] , \tag{A2}$$

$$N_{0j(m)}^{(p)} = i(R_{00}^{m} + R_{jj}^{m})[\Omega_j^S(\rho_{j0(m)}^{(p)} - \rho_{0j(m)}^{(p)}) + \Omega_j^N \rho_{j0(m-n)}^{(p-1)} - \Omega_j^{N*}\rho_{0j(m+n)}^{(p-1)}]$$
$$+ iR_{00}^{m}[\Omega_{3-j}^S(\rho_{3-j0(m)}^{(p)} - \rho_{03-j(m)}^{(p)}) + \Omega_{3-j}^N \rho_{3-j0(m+n)}^{(p-1)} - \Omega_{3-j}^{N*}\rho_{03-j(m-n)}^{(p-1)}] + [R_{00}^0 \Lambda_0 - R_{11}^0 \Lambda_1]\delta_{p,0} , \tag{A3}$$

$$\rho_{12(m)}^{(p)} = iR_{12}^{m}[\Omega_1^S \rho_{02(m)}^{(p)} + \Omega_1^{N*} \rho_{02(m+2)}^{(p-1)} - \Omega_2^S \rho_{10(m)}^{(p)} - \Omega_2^N \rho_{10(m+2)}^{(p-1)}] , \tag{A4}$$

$$\rho_{21(m)}^{(p)} = -iR_{21}^{m}[\Omega_1^S \rho_{20(m)}^{(p)} + \Omega_1^N \rho_{20(m-2)}^{(p-1)} - \Omega_2^S \rho_{01(m)}^{(p)} - \Omega_2^{N*} \rho_{01(m-2)}^{(p-1)}] , \tag{A5}$$

where $n = 2\delta_{j,1} - 2\delta_{j,2}$, $R_{ij}^{m} = (R_{ji}^{-m})^* = (L_{ij}^{m})^{-1}$, and

$$L_{ij}^{m} = \tfrac{1}{2}(\gamma_i + \gamma_j) + \Gamma_{ij}^C + i[\Delta_i - \Delta_j + (m - \mu_i^S + \mu_j^S)Kv] \tag{A6}$$

with $\Gamma_{ii}^C = \Delta_0 = 0$.

These equations, valid for $p \geq 0$, relate the coefficients of a given order p and $\pm n$ only to those of order $p - 1$ and $\pm n \pm 2$. Since the zero-order solution corresponds to $p = 0$ and $m = 0$, the only nonzero Fourier coefficients are those with $|m| \leq 2p$.

The zero-order Fourier components of the population differences $N_{0j}^{(0)} = \rho_{00}^{(0)} - \rho_{jj}^{(0)}$ basically characterize the strong pump coupling and resultant coherent population effects in the mixing process. Resolution of the closed set of Eqs. (A1)–(A5) for $p = m = 0$ is straightforward and gives

$$N_{0j(0)}^{(0)} = \frac{N_{0j}^e(1 - F_{3-j,3-j}) - N_{03-j}^e F_{j,3-j}}{(1 - F_{j,j})(1 - F_{3-j,3-j}) - F_{j,3-j}F_{3-j,j}} , \tag{A7}$$

being the equilibrium population differences $N_{0j}^e = P_j = \Lambda_0/\gamma_0 - \Lambda_j/\gamma_j$, and

$$F_{ij} = 2|\Omega_j^S|^2 \mathrm{Re}\{H_{ij}/D^0\} , \tag{A8}$$

$$D^0 = L_{12}^0 L_{10}^0 L_{02}^0 + |\Omega_1^S|^2 L_{10}^0 + |\Omega_2^S|^2 L_{02}^0 , \tag{A9}$$

$$H_{11} = \frac{|\Omega_2^S|^2}{\gamma_0} - \frac{L_{21}^0 L_{20}^0 + |\Omega_1^S|^2}{\gamma + \gamma_0} , \tag{A10}$$

$$H_{22} = \frac{|\Omega_1^S|^2}{\gamma_0} - \frac{L_{21}^0 L_{01}^0 + |\Omega_2^S|^2}{\gamma + \gamma_0} , \tag{A11}$$

$$H_{12} = \frac{L_{21}^0 L_{01}^0 + |\Omega_2^S|^2}{\gamma_0} - \frac{|\Omega_1^S|^2}{\gamma_0 + \gamma} , \tag{A12}$$

$$H_{21} = \frac{L_{21}^0 L_{20}^0 + |\Omega_1^S|^2}{\gamma_0} - \frac{|\Omega_2^S|^2}{\gamma_0 + \gamma} . \tag{A13}$$

Introducing the detuning-dependent saturation parameters

$$I_j^D = I_j/[1 + (\delta_j^\mu)^2], \quad \mu = \mu_j^S \tag{A14}$$

and

$$I_j^C = I_j/[1 + (\delta_{3-j}^\mu)^2], \quad \mu = \mu_{3-j}^S , \tag{A15}$$

where μ_j^S, δ_j^μ, and I_j are respectively defined by Eqs. (2), (22), and (25), Eqs. (A8)–(A13) explicitly yield

$$F_{jj} = -2I_j^D(1 + r) + 2I_1^D I_2^D \mathrm{Re}\{[A_j(r + 1) + rB]/Z\} , \tag{A16}$$

$$F_{j3-j} = 2I_{3-j}^D r - 2I_1^D I_2^D \mathrm{Re}\{[B(r + 1) + rA_{3-j}]/Z\} , \tag{A17}$$

where the pump-coupling terms, proportional to $I_1^D I_2^D$, are characterized by

$$B = (1 - i\delta_2^+)(1 + i\delta_1^-) , \tag{A18}$$

$$A_1 = (1 + i\delta_1^-)[1 + (\delta_2^+)^2]/(1 - i\delta_1^-) , \tag{A19}$$

$$A_2 = (1 - i\delta_2^+)[1 + (\delta_1^-)^2]/(1 + i\delta_2^+) , \tag{A20}$$

$$Z = 1 + C - \frac{i\Gamma}{\gamma}(\delta_1^- - \delta_2^+) + I_1^C(1 - i\delta_2^+) + I_2^C(1 + i\delta_1^-) . \tag{A21}$$

C and r are the relaxation parameters defined by Eqs. (24) and (26).

In the EZCA approximation, coherent population trapping effects due to pump-field coupling are neglected, owing to their negligible incidence in the Doppler limit. These effects are accounted for in F_{jj} and F_{j3-j} through the $I_1^D I_2^D$ terms, which manifest a high velocity dependence through Z. Dropping them out, the population differences are described by

$$N_{0j(0)}^{(0)} = \frac{N_{0j}^e[1 + 2(1 + r)I_{3-j}^D] - N_{03-j}^e 2rI_{3-j}^D}{[1 + 2(1 + r)I_j^D][1 + 2(1 + r)I_{3-j}^D] - 4r^2 I_{3-j}^D I_j^D} \tag{A22}$$

and result for $r \ll 1$ in the very simple expression

$$N_{0j(0)}^0 = \frac{N_{0j}}{1 + 2I_j^D} . \tag{A23}$$

[1] See, e.g., *Optical Phase Conjugation,* edited by R. A. Fisher (Academic, New York, 1983).

[2] P. F. Liao, D. M. Bloom, and N. P. Economou, Appl. Phys. Lett. **32**, 813 (1978).

[3] M. Kauranen and R. W. Boyd, Phys. Rev. A **44**, 584 (1991).

[4] G. P. Agarwal, Phys. Rev. A **28**, 2286 (1983).

[5] J. Mlynek, F. Mitschke, E. Köster, and W. Lange (unpublished); E. Köster, J. Mlynek, and W. Lange, Opt. Commun. **53**, 53 (1985).

[6] R. Saxena and G. S. Agarwal, Phys. Rev. A **31**, 877 (1985).

[7] S. Le Boiteux, P. Simoneau, D. Bloch, F. A. M. de Oliveira, and M. Ducloy, IEEE J. Quantum Electron. **QE-22**, 1229 (1986).

[8] M. Pinard, P. Verkerk, and G. Grynberg, Phys. Rev. A **35**, 4679 (1987).

[9] F. A. M. de Oliveira, C. B. de Araujo, and J. R. R. Leite, Phys. Rev. A **38**, 5688 (1988).

[10] C. Schmidt-Iglesias, G. Orriols, and F. Pi, Appl. Phys. B **47**, 27 (1988).

[11] T. Fu and M. Sargent III, Opt. Lett. **5**, 433 (1980).

[12] N. Chencinski, W. M. Schreiber, A. M. Levine, and Y. Prior, Phys. Rev. A **42**, 2839 (1990).

[13] C. Parigger, P. Hannaford, W. J. Sandle, and R. J. Ballagh, Phys. Rev. A **31**, 4043 (1985).

[14] D. J. Gauthier, M. S. Malcuit, A. L. Gaeta, and R. W. Boyd, Phys. Rev. Lett. **64**, 1721 (1990).

[15] B. Ya Zel'dovich and V. V. Shkunov, Kvant. Elektron. (Moscow) **6**, 629 (1979) [Sov. J. Quantum Electron. **9**, 379 (1979)]; G. Martin, L. K. Lam, and R. W. Hellwarth, Opt. Lett. **5**, 185 (1980).

[16] J. F. Lam and R. L. Abrams, Phys. Rev. A **26**, 1539 (1982).

[17] S. M. Wandzura, Opt. Lett. **4**, 208 (1979).

[18] M. Ducloy and D. Bloch, Opt. Commun. **47**, 351 (1983).

[19] J. F. Lam, D. G. Steel, R. A. McFarlane, and R. C. Lind, Appl. Phys. Lett. **38**, 997 (1981).

[20] S. N. Jabr, L. K. Lam, and R. W. Hellwarth, Phys. Rev. A **24**, 3264 (1981).

[21] P. P. Berman, D. G. Steel, G. Khitrova, and J. Liu, Phys. Rev. A **38**, 252 (1988).

[22] Y. H. Zou and N. Bloembergen, Phys. Rev. A **33**, 1730 (1986); *ibid.* **34**, 2968 (1986).

[23] G. Alzetta, in *Coherence in Spectroscopy and Modern Physics,* edited by F. T. Arrecchi, R. Bonifacio, and M. O. Scully (Plenum, New York, 1978); G. Orriols, Nuovo Cimento B **53**, 1 (1979).

[24] H. R. Gray, R. M. Whitley, and C. R. Stroud, Jr., Opt. Lett. **3**, 218 (1978).

[25] H. J. Yoo and J. H. Eberly, Phys. Rep. **118**, 239 (1985).

[26] D. Bloch and M. Ducloy, J. Opt. Soc. Am. **73**, 635 (1983); **73**, 1844 (E) (1983).

[27] M. S. Feld and A. Javan, Phys. Rev. **177**, 540 (1969).

[28] S. Haroche and F. Hartmann, Phys. Rev. A **6**, 1280 (1972).

[29] M. S. Feld, M. M. Burns, T. U. Kühl, P. G. Pappas, and D. E. Murnick, Opt. Lett. **5**, 79 (1980).

[30] A. Yariv and D. M. Pepper, Opt. Lett. **1**, 16 (1977); R. L. Abrams and R. C. Lind, *ibid.* **2**, 94 (1978); **3**, 205 (1978).